

Leong, K. H., Sabo, K. R. and Albright, C. E.
Laser beam welding of 5182 aluminum alloy sheet.
J. Laser Applications, 11: (3) 109-118 Jun. 1999.

Laser Beam Welding of 5182 Aluminum Alloy Sheet

K. H. Leong^{1*}, K. R. Sabo^{1#}, B. Altshuller², T. L. Wilkinson^{3**} and Charles E. Albright⁴

¹Argonne National Laboratory, ²Alcan International Limited,

³Reynolds Metals Company¹, ⁴Ohio State University

Abstract

Conditions were determined for consistent coupling of a CO₂ laser beam to weld 5182 aluminum alloy sheet. Full penetration butt and bead-on-plate welds on 0.8 and 1.8 mm sheets were performed. Process conditions examined included beam mode, spot size and irradiance, shielding gas flow, and edge quality and fitup. The observed weld quality variations with the different process parameters were consistent with physical phenomena and a threshold irradiance model. Optimal conditions were determined for obtaining consistent welds on 5182 alloy sheets. Formability and tensile tests were performed on the welded samples. All test failures occurred in the fusion zone. Reduction in formability and tensile strength of the welded samples are discussed with respect to weld profiles and process parameters.

Keywords: aluminum, laser beam welding, process parameters, threshold irradiance

Introduction

Use of lightweight materials improves the energy efficiency and fuel economy of automotive vehicles. An aluminum intensive midsize American sedan could potentially be 20% lighter than the standard steel based vehicle. This decrease in weight translates into a 12% improvement in fuel economy [1]. Economically substituting aluminum for steel in body and chassis components is difficult. It is more cost effective to design a part specifically for aluminum, taking advantage of its design flexibility and specific stiffness. Aluminum alloys have a higher thermal conductivity and higher reflectivity, which make welding more difficult than welding steel. Improvements to conventional welding practices are needed to enhance the welded properties of aluminum joints.

This paper examines laser beam welding which has been identified as a promising method for joining aluminum in body applications such as tailored blanks. Initial efforts by other researchers applied previous experience with steel to aluminum but the process parameters

*Currently at Penn State Applied Research Lab

#Currently at Lockheed Martin Atlanta

**Currently at M. H. West & Co.

developed for steel did not produce good welds [3]. Later work with a better fundamental understanding of the welding process showed the need for a higher irradiance beam to produce welds on aluminum alloys [4]. Laser power is not the appropriate parameter as the energy/heat flux from the laser beam to the metal is determined by the irradiance. The high reflectivity of aluminum alloys for the laser radiation together with the high thermal conductivity increases the required threshold irradiance to initiate melting and the formation of a keyhole. Experimental attempts to correlate the threshold irradiance with the thermal conductivity of the alloy showed no clear trends [4,5,6]. Rapp et al. showed that alloying element volatility also affected the threshold irradiance [5]. Further work by Leong et al. led to the development of a simple equation that predicts the threshold irradiance for melting and correlated the effects of the metal absorptivity, thermal conductivity and temperature increase for melting, beam diameter and welding speed [7].

An abundance of publications exist on the laser welding of aluminum alloys [see 8, 9]. Most of the research are somewhat empirical in their approach and tend to report observations without precise process parameters (caused by lack of diagnostic instrumentation) or adequate explanation of the underlying physical phenomena. Recent efforts have reported more precise data with improvements in instrumentation. The intent of this paper is to research the interaction of a CO₂ beam with 5182 aluminum alloy to obtain data under controlled conditions that will be applicable to industrial welding applications such as in the welding of tailored blanks. In addition, underlying physical phenomena that may have significant effects on the welding process are also elucidated.

Experimental Procedures

Aluminum alloy 5182-O was selected for this work because it is a laser weldable alloy and is a potential candidate for automotive body applications. The nominal alloying elemental composition is listed in Table 1. Flat stock (0.8 and 1.8 mm) were provided by Alcan International Limited and Reynolds Metals Company. All samples were wiped with acetone immediately prior to welding. Butt welds were made on shear cut edges with dry shearing blades.

Welds were carried out with a rf-excited CO₂ laser (Rofin-Sinar RS6000). Near TEM₀₀ ($M^2=1.2$) and near TEM₂₀ ($M^2=4.2$) beams were used for the investigation. Reflective optics were used for beam delivery. The raw beam that was polarized 45° to the horizontal exited the laser horizontally. A mirror with a 1/4 wave coating was used to bend the beam vertically and also produce a circularly polarized beam. The optics system mounted on the z-axis has a rotatable stage where different beam shaping components can be attached. All welds in this study was carried out with a 15° tilt in the focussing optic to prevent backreflection into the resonator. If proper process parameters are used, this tilt that reduces the normal irradiance on the workpiece surface is unnecessary. A 206 mm (8.1 in) Spawr focus module and off-axis parabolas of 125 mm and 150 mm focal lengths were used to produce different spot sizes. A Spawr cross-flow system was used to prevent spatter on the optics. Beam irradiances were measured with a beam analyzer (Prometec UFF100) with the beam propagating in the vertical as shown in Fig. 1. The incident irradiance at 15° on a horizontal sample will be approximately 3.4% lower than that obtained with the beam analyzer. Since this difference is small, the

reported values are not adjusted. Beam radii reported here are the 86% energy values. The beam power was measured with a digital power probe (Macken Instruments).

A x-y table was used to move the workpiece and was controlled by a CNC (Fanuc). Inert gas shielding was obtained with a 4.5 mm ID tube oriented at 35° or 40° to the horizontal or using a coaxial gas flow welding nozzle. High purity helium (99.995%) was used with a flowrate of 28 lpm (100 cfh) for top shielding. Bottom shielding (37 lpm of helium) for butt welds was through a steel tube 12 cm long with a hole every 1 cm. The bottom shielding was fixtured to the z-axis to maintain shielding configuration during welding. Alignment of the CO₂ beam to the butt joint was obtained using the laser system HeNe laser that has been determined to be aligned with the CO₂ beam position to within 0.5 mm. All samples for butt and bead-on-plate (BOP) welds were wiped with acetone prior to welding unless stated otherwise. Welds of 100 mm length were performed. Welds up to 610 mm were also obtained.

Weld profiles were obtained by sectioning and polishing selected samples. Weld samples were etched with Kellers reagent to reveal inclusions and increase the contrast of the fusion zone with the base metal. Weld hardness profiles were obtained with a microhardness tester fitted with a Knoop indenter (200 g) calibrated to meet ASTM E-384. Edge fitup was examined after tack welding every other inch. The “tack” welds were mounted in bakelite, polished and examined under a microscope.

254 mm butt welds were produced on 1.8 mm sheets resulting in a 254 mm x 203 mm welded section. Edge preparation used included shear-cut, shear-cut with wire brushing, and dry-mill. Duplicate welds were carried out for tensile and formability tests. For some of the later welds, 50 mm of the 254 mm weld was removed for tensile tests transverse to the welding direction. Five tensile tests were carried out for each weld by Reynolds Metals Company. Hemispherical punch stretching tests were carried out by Alcan International. Tests were performed with the root of the weld in contact with the punch at a punch speed of 25.4 mm/min. The clamping load was at 400 kN with the weld position at the center of the punch. The strain path was at or near balanced biaxial and a new 4mm thick polyurethane pad was used for lubrication.

Threshold Irradiance

Threshold irradiance tests have conventionally been performed on clean samples so that repeatable results are obtained. For aluminum alloys, surfaces have varying degrees of oxidation and lubricants applied in the manufacturing process. Consequently, data obtained from consistently clean and oxide free surfaces may not be applicable to the manufacturing environment. Figure 3 shows the results of beam coupling tests on a sample of 5182 alloy. Leading edge cross jet configuration (see Fig. 5a) was used for all threshold irradiance tests. Attempted welds were made with the TEM₀₀ beam (200 μm focused diameter) from left to right using increasing beam irradiance but at a fixed traverse speed. The results show that as the irradiance is increased, the scribing changes from intermittent to consistent welds at irradiances >2.7 MW cm⁻². Attempted welds with the TEM₂₀ beam (400 μm focused beam diameter) produced similar trends but consistent welds were produced at irradiances >2.3 MW cm⁻². The model of Leong et al. for the irradiance necessary for melting has

$$I_m = \frac{k(T_{\text{melt}} - T_0)}{AdJ_{\text{max}}} \quad (1)$$

where k is the thermal conductivity of the metal, $(T_{\text{melt}} - T_0)$ is the difference in melting and ambient temperature, A is the absorptivity of the surface, d is the diameter of the beam at the surface and J_{max} is a function of the ratio of the thermal diffusivity to the product of the traverse speed and diameter of the incident beam [7]. Using a value of 5% for the absorptivity and a traverse speed of 12.7 ms^{-1} , the irradiance values for melting are computed to be 2.7 MW cm^{-2} and 1.3 MW cm^{-2} for the $200 \text{ }\mu\text{m}$ and $400 \text{ }\mu\text{m}$ beam diameter cases respectively. The model has been shown to provide good lower bound guides for welding threshold irradiance. Noting that the absorptivity value is an approximation and does not account for oxidation at the surface, the experimental data and the predicted values are consistent in trend of higher irradiance for smaller spot sizes of the beam.

The data obtained with both beam modes for attempted BOP and butt welds are shown in Fig. 4 which has irradiance as a function of beam power. The BOP and butt weld data is not differentiated in Fig. 3 as the symbols are already cluttered but details are available in Sabo's thesis [9]. Beam powers $<2 \text{ kW}$ are for TEM00 beam data and higher beam powers are for TEM20 data. Irradiances that produced scribing or inconsistent welds are indicated by "uncoupled" and consistent welds by "coupled". The threshold irradiances for consistent welds for the two different beam sizes are indicated by horizontal lines in the figure. The value for the TEM00 beam data is 2.8 MW cm^{-2} and for the TEM20 data is 2.3 MW cm^{-2} . These values are consistent with a threshold irradiance of 2 MW cm^{-2} obtained by Sakamoto et al. for a 4.9 wt. % Mg aluminum alloy. Above the threshold irradiance line, all attempted welds produced consistent welds. Below the line, attempted welds produced inconsistent or no welds. At lower irradiances, i.e., $<2.4 \text{ MW cm}^{-2}$ for the TEM00 BOP data and $<2.0 \text{ MW cm}^{-2}$ for the TEM20 data no welds were produced. The TEM00 butt weld data indicate a substantially lower threshold irradiance than the BOP data with consistent welds obtained for irradiances as low as 1 MW cm^{-2} . This anomaly is caused by some data obtained using a defocussed beam with beam diameters of 300 to $400 \text{ }\mu\text{m}$ at the surface and beam trapping in between the edges of the butt [10-12]. Data obtained with BOP welds showed a decrease in irradiance for coupling from 2.9 MW cm^{-2} for a beam size of $192 \text{ }\mu\text{m}$ to 1.8 MW cm^{-2} for a beam size of $300 \text{ }\mu\text{m}$ [see data in 9]. This agrees with the prediction of Eqn. 1 for the increase in beam size. However, the lowest irradiance for coupling obtained is 1 MW cm^{-2} . The lower irradiance observed is attributed to the beam trapping effect. A typical gap between shear-cut edges is shown in Fig. 5. The top of the gap for this particular case is approximately $160 \text{ }\mu\text{m}$ which is comparable to the spot size of the TEM00 beam. Consequently, the beam trapping effect would be dependent on alignment of the beam with the gap. For the TEM20 beam that has a $400 \text{ }\mu\text{m}$ spot size, the effect of beam trapping would be substantially diminished because the gap is $<25\%$ of the total beam area. The beam alignment effect would also be diminished. Hence, no significant decrease in threshold irradiance was observed for butt welds with the larger TEM20 beam. With the above considerations, the threshold irradiances indicated in Fig. 4 are applicable to BOP and butt welds

with good fitup and where fitup tolerances are small compared to beam spot size.

Gas Shielding Effects

The different gas shielding configurations illustrated in Fig. 6 were used to determine top shielding effects on weld appearance. The slightly different angles were necessitated by constraints in the experimental system and fixturing limitations but do not produce significant differences in results. Beam focus was located at the workpiece surface. The different cross jet configurations affect the plasma formation over the weld. The leading edge configuration tends to blow plasma to the to-be-welded location while the trailing edge and transverse direction configurations blow the plasma away from the to-be-welded location. The presence of plasma tends to absorb and defocus the beam. Unpublished tests by the authors on steel parts have shown that weld penetration is decreased using the leading edge configuration. The results obtained for aluminum using the TEM₂₀ beam at 5.1 kW and a weld speed of 12.7 ms⁻¹ also show a decreased penetration for the leading edge case. The coaxial flow configuration is not as efficient in “blowing” away the plasma as a side jet and also produced lower weld penetration. The decreased penetrations obtained by the leading edge and coaxial flow cases are evident in the weld bottom profile where intermittent full penetration occurred resulting in a spiky surface as shown in Fig. 7. Increasing beam power reduced areas of incomplete penetration for the leading edge cross jet case but still produced a spiky underbead. The orientation of the gas jet blowing into the keyhole in the direction of the advancing melt zone may have contributed to weld root instability. Welds obtained with the same process parameters but with the trailing edge and transverse flow configurations resulted in full penetration welds and a relatively smooth underbead as shown in Fig. 8. Similar results for the welds were also obtained for the TEM₀₀ case.

Mixtures of argon and helium were also used for top shielding to assess the effects. Berkmanns et al have found that the addition of argon aids in the welding process [13]. However, in this work where irradiance is carefully controlled, we have found that the addition of (up to 50%) argon tends to decrease weld penetration but does not increase weld quality.

In addition to surface features, distinct color differences were observed for the different cross jet configurations. Leading edge and transverse configurations resulted in shiny silver top weld surfaces but trailing edge and coaxial flow resulted in gray surfaces. For the transverse flow configuration, the surface just removed from the weld and downstream of the jet had a coating of a black powder. Analysis by energy dispersive x-ray spectroscopy (EDS) revealed that the black powder and grey coating on the weld surface was composed of mostly magnesium and oxygen. Scanning electron micrographs of the two welds with the positions analyzed are shown in Fig. 9. The accelerating voltage was set at 5 kV to minimize penetration into the sample surface. The results are shown in Table 2. The base metal magnesium content of 9.7% indicated is higher than for 5182 alloy. The high base metal content of oxygen is probably from surface oxidation which occurs readily for aluminum [14]. Although the EDS technique tends to be somewhat qualitative, relative comparison of the results indicates loss of magnesium from the fusion zone. The high oxygen content associated with high magnesium probably arose from the oxidation of the vaporized magnesium when air entrainment occurred. The low oxygen content at low magnesium values in the fusion zone together with the silvery appearance indicate good

shielding.

EDS analysis was also performed on the weld metal to assess overall magnesium loss. No significant loss within the precision of the technique was found. Other researchers had obtained similar results using beams of similar or lower powers [e.g. 15]. However, it is evident that there is some loss of magnesium to produce the dark powder on the surface but not substantial enough to make a difference considering the imprecision of the EDS technique. At higher beam powers and larger beam spot sizes at slower weld speeds, magnesium loss from the weld metal has been found [16, 17]. The longer interaction at slower weld speeds will tend to increase magnesium loss.

Location of Beam Focus

Most of the data reported here are obtained using a beam focus position at or above (~2.5mm) the workpiece surface. Martukanitz, et al. found that using beam defocusing produced better welds and avoided hole formation but beam irradiances were not measured precisely [18, 19]. Park et al. located beam focus below the surface and obtained good welds. We have observed that locating the beam focus inside the weld increased the welding efficiency in that substantially higher weld speeds (16.9 instead of 12.7 ms⁻¹) can be used to obtain the same penetration if the irradiance is controlled. The effect of high irradiance on weld quality will be discussed in the next section.

Weld Quality

Laser welding of aluminum tends to produce a higher degree of spatter than for the case of steel. A higher cross-flow was necessary to prevent spatter on the optics. High irradiances also tend to produce more spatter and lower weld surface quality for aluminum. Typical weld cross sections for butt welds obtained using the 6 in focal length parabola with transverse cross jet configuration are shown in Figs. 9 and 10. The spot sizes at focus were 200 and 400 μm for the TEM₀₀ and TEM₂₀ beams respectively. Beam focus was located at the workpiece surface. The voids/porosities in the weld cross sections tend to be relatively small with a few larger voids. All voids were smaller than 0.1 mm. The welds obtained with the TEM₀₀ beam tend to have higher porosity. The irradiances used here were very similar for both beam modes. The narrower welds higher porosity could result from the smaller surface area and more constrained convection of the weld pool for expulsion of gases produced. All weld cross sections examined showed some degree of porosity regardless of edge preparation. Dry milled or wire-brushed edges had similar levels of porosity.

Fitup of the edges tend to cause a problem with the weld nugget shape, being more severe with the narrower welds (see Figs. 9 and 10). As is well known, fitup is more critical with thinner gage material and improved fixturing should produce better weld shapes.

The hardness profile across a typical butt weld from shear cut edges obtained with the TEM₂₀ beam is shown in Fig. 11. The average Knoop hardness of the base metal was 80±5 KHN. The average hardness of the weld metal was 82±6 KHN with a small increase in hardness near the edge of the fusion zone. The heat affected zone could not be distinguished from the etched weld

cross-section. 5182-O alloy is a non-heat-treatable alloy in the annealed condition. The metal does not depend on precipitation strengthening and therefore is not susceptible to overaging. The EDS analysis and the presence of magnesium powder on the surface indicated a relatively small loss in magnesium. Substantial loss of magnesium would cause a decrease in hardness. The rapid cooling rates characteristic of laser welding tends to result in smaller grain sizes that may have some effect on the hardness. The hardness data indicate a small increase in the weld metal similar to results obtained with 5754-O alloy [18, 19].

Martukanitz et al. have found that high beam irradiance can lead to cavity defects for aluminum alloys that have low surface tension and viscosity in the molten state. Holes or voids would form in the weld from cavitation. Use of lower irradiance, but greater than the threshold value, tends to reduce cavity defects [18, 19]. This observation contrasts with the finding that higher irradiance tends to reduce porosity in welds on steel [20, 21]. The surface tension and viscosity of iron at the melting point are 1.9 Nm^{-1} and 5.5 Pa-s compared to 0.9 Nm^{-1} and 1.3 Pa-s for aluminum [22]. The high surface tension and viscosity of steel may require higher irradiance to increase weld pool convection for release of gas bubbles whereas higher irradiance for aluminum creates more gas bubbles with an already unstable weld pool. Higher spatter as observed for aluminum would be expected for the case of lower surface tension and viscosity alloys with less stable weld pools. Butt welds carried out in this study with 1.8 and 0.8 mm thick material provided more data on this problem of cavity defects. Full penetration butt and BOP welds were performed on sheet thicknesses of 0.8 and 1.8 mm with different beam modes and spot sizes. The results are shown in Table 3. The data for the 0.8 mm sheet indicate that wider welds are more susceptible to cavity defects. No holes were observed for the 1.8 mm sheet. These results are consistent with a relatively low surface tension fluid where dropout of molten material would be more frequent with wider weldpools. The thicker sheet will provide more adhesion on the sidewalls to hold up the weldpool and also affect (constrain) the weldpool dynamics resulting in less hole formation for the same weld width.

Formability and Tensile Strength

The results of the tests are tabulated in Tables 4 and 5. The later results (under new fixture) in Table 4 and all results in Table 5 were obtained from welds performed with an improved fixturing setup using a thick aluminum plate with a groove machined on the surface for bottom gas shielding and precision machined surfaces. For the formability and tensile tests all fractures occurred in the weld metal. This is not unexpected with the slight loss in magnesium and undercut present.

For the old fixture case, dome heights obtained with the TEM₂₀ beam for the shear-cut (6 welds) and wire brush after shear-cut (2 welds) prepared edges varied from 14 to 23 mm at fracture with an average value of 19. The dome heights for the dry-mill case (4 welds) were significantly higher from 25 to 31 mm with an average value of 28 mm. Alcan states a requirement of 26 mm for automotive body applications [23]. For the TEM₀₀ case, dome heights for shear-cut and wire brush edges varied from 17 to 28 mm with an average of 23.2 mm and the dry mill values varied from 18.1 to 27.5 mm with an average value of 24. Examination of the fitup for the different edge preparations indicate that the dry-mill case had good fitup whereas the other cases had some mismatch of the edges arising from the slight curvature from the action of shearing and

the simple clamping fixture used (see Figs. 4 and 5). The poor fitup and any undercut would tend to decrease weld size (thickness) and strength, and formability. The use of narrower beams would place more stringent requirements on fitup but the results obtained show no significant difference in dome heights. The weld profile obtained with the TEM₀₀ beam as indicated in Fig. 9 shows a relatively large lower bead that masks any difference in fitup. The ultimate tensile stress, yield stress and elongation exhibited similar trends as the formability. For the old fixture and TEM₂₀ case, the shear-cut and wire brush values range from 178 to 200 MPa for ultimate tensile stress, 95 to 113 MPa for yield stress and 6.3 to 7.4 % for elongation with average values of 189 MPa, 106 MPa, and 7.2% respectively. The dry mill case had corresponding average values of 216 MPa, 105 MPa and 10.7%. The Aluminum Association's minimum values for 5182-0 are 255 Mpa, 110 MPa, and 18% [24]. The data indicate that improved fitup would lead to better weld profile and higher tensile strength consistent with the formability results. The TEM₀₀ tensile tests did not show significant differences for different edge quality.

Results obtained using the improved fixturing show improved tensile strength for shear cut edges but with no improvement in formability. There appears to be some loss in formability and tensile strength at lower weld speeds that would increase magnesium loss.

Occurrence of oxides were prevalent on some welds and may have affected formability. An improved inert gas shroud was developed to prevent any entrainment of ambient air that occurred when a gas jet is used. This new gas shielding method required normal incidence of the beam in contrast to the previous data obtained with the beam at 75° to the horizontal. More efficient welding was achieved with this geometry with lower beam power and irradiance at the same weld speed. The dome height varied from 15.5 to 21.1mm with an average of 19.4mm. The ultimate tensile stress varied from 232 to 269 MPa with an average of 251 MPa and the elongation varied from 7.7 to 13.6% with an average of 10.4%. Improved fixturing and lower irradiance (lower magnesium loss) resulted in improved tensile strength but not for formability. Examination of the weld profiles for this geometry and process conditions showed the presence of undercut and occasional dropout which will decrease both formability and tensile strength.

Summary and Discussions

Details provided in this work on aluminum alloy 5182 together with results obtained by other researchers on aluminum alloys reveal that CO₂ laser beam welding of aluminum alloys has limitations in obtaining the desired weld strength and formability required for automotive applications. In particular, for 1.8 mm 5182 aluminum alloy samples with shear cut edges, butt welds obtained with CO₂ beams achieved ultimate tensile strength of 251 MPa, elongation of 10.4% and 75% of desired formability in terms of dome height. Martukanitz et al. results had corresponding values of 190 MPa, 5.4% and 77% respectively [19].

Martukanitz used a defocused beam with higher power (6.6 kW) and spot size. Loss of magnesium may have been higher with the higher power used at similar weld speed (12.7 cms⁻¹). The high irradiance required of CO₂ beams for welding will produce some magnesium loss with resulting reduction in weld bead strength. In addition, undercut and cavity defects or porosities will further reduce material strength and formability. Molten aluminum with its low

surface tension and viscosity is particularly susceptible to undercut and cavity defects at high beam irradiance. A partial solution to this problem is to use the Nd:YAG laser beam that is better absorbed by aluminum resulting in lower required irradiance. Martukanitz and Altshuler has obtained butt weld profiles on shear cut 5754 alloy samples that have minor undercut and weld root reinforcement [25]. Weld bead appearance was more consistent compared to CO₂ welds with no evidence of cracks or cavity defects. However, only a small improvement (5%) in tensile strength was obtained but there was a reduction in elongation from 15% to 11% compared to the CO₂ case. A formability of 70% of parent metal was obtained. Use of filler wire for CO₂ beam welding increases tensile strength of the weld bead through material reinforcement but formability is still impaired compared to the parent material [13, 19].

Analysis of data on laser beam welding of aluminum alloys indicates that loss of volatile alloying elements such as magnesium for strengthening can be minimized by decreasing beam irradiance and interaction time (i.e., increasing weld speed). The use of the shorter wavelength Nd:YAG laser beam with increased absorption by aluminum lowers the irradiance required to weld and has the added benefit of producing a more stable weld pool and consistent welds. However, more optimal conditions need to be determined to maximize the formability.

An important result achieved in this work is that the critical parameters in the laser welding process to obtain consistent welds have been reduced to controlling the beam irradiance. Special edge preparation, gas blending or nozzles are unnecessary for consistent welds. This finding where only one critical parameter (good fitup is always necessary) needs to be controlled improves the robustness of laser beam welding of aluminum in industrial applications.

Acknowledgement

This work was supported in part by the U.S. Department of Energy, Office of Energy Research Laboratory Technology Research Program and the Office of Advanced Automotive Technologies. The paper is based on the M.S. Thesis (Ohio State University) of Ken Sabo who was a Laboratory-Graduate Participant in a program administered by the Argonne Division of Educational Programs with funding from the U.S. Department of Energy.

References

1. Stodolsky, F., A. Vyas, R.Cuenca, and L. Gaines. "Life-cycle energy savings potential from aluminum-intensive vehicles." SAE Technical Paper Series 951837, Proceedings of the 1995 Total Life Cycle Conference (P-293).
2. Noel, J. M. An overview of tailored-blanks and preliminary design guidelines. Proceedings Automotive Laser Applications Workshop (ALAW'94), Dearborn, Michigan, March 7-8, 1994.
3. Mazumder, J. Laser welding: state of the art review. J. Metals July 1982, 16-24,.
4. Sakamoto, H., K. Shibata, and F. Dausinger. "Laser welding of different aluminum alloys." Proceedings of Laser Materials Processing Symposium (ICALEO'92), October 25-29, 1992, Orlando, Florida, pp. 523-28,.

5. Rapp, J., M. Beck, F. Dausinger, and H. Hügel. "Fundamental approach to the laser weld ability of aluminum and copper alloys." ECLAT'94. Proc. 5rd European Conf. on Laser Treatment of Materials, Bremen-Vegesack, Germany, September 26-27, 1994, pp. 313-325,.
6. Mehmetli, B. A., K Takahashi, and S. Sato. "Comparison of aluminum alloy welding characteristics with 1 kW CO and CO₂ lasers." J. Laser Applications, 8, 1996, pp. 25-31.
7. Leong, K. H., H. K. Geyer, K. R. Sabo, and P. G Sanders. "Threshold laser beam irradiances for melting and welding." J. Laser Applications, 9, 1997, pp. 227-232.
8. Leong, K. H., K. R. Sabo, P. G. Sanders, and W. J. Spawr. "Laser beam welding of aluminum alloys", SPIE Proceedings Vol. 2993 Lasers as Tools for Manufacturing II, 1997.
10. Huntington, C. A. and T. W. Eagar. "Laser welding of aluminum and aluminum alloys." Welding Journal, 62(4), 1983, pp. 105s-107s,.
11. Arata, Y. "Narrow gap high energy density beam welding - principle," Plasma, Electron and Laser Beam Technology, ASM International, 1986.
12. K. H. Leong, D. J. Holdridge, M. G. Seibert and D. E. Nelson (1994) "High Speed Laser Welding
13. J. Berkmanns, R. Imhoff, K. Behler and E. Beyer. "Laser welding of aluminum." Proceedings Automotive Laser Applications Workshop (ALAW'95), Dearborn, Michigan, March 6-
14. Wakefield, G. R. and R. M. Sharp. "The composition of oxides formed on Al-Mg alloys. Applied Surface Science," 51, 199, pp. 95-102.
15. Pak, S. W., K. H. Kim, S. Y. Kwon, and W. S. Cho. "A study on the joining technology of aluminum
16. Blake, A. and J. Mazumder. "Control of magnesium loss during laser welding of Al-5083 using a plasma suppression technique." Journal of Engineering for Industry, 107(8), 1983, pp. 275-280,.
17. Moon, D. W. and E. A. Metzbower. "Laser beam welding of aluminum alloy 5456." Welding Journal, 62(2), 1983, pp. 53s-58s.
18. Martukanitz, R. P., D. J. Smith, F. G Armao, A. Baldantoni, and E. R. Pickering. "Laser beam welding of aluminum alloys for automotive applications." Proceedings of the Society of Automotive Engineers International Congress and Exposition, February 28-March 3, 1994, Detroit, Michigan.
19. Martukanitz, R. P., B. Altshuller, F. G. Armao, and E. R. Pickering. "Properties and characteristics of laser beam welds of automotive aluminum alloys." Proceedings of the Society of Automotive Engineers International Congress and Exposition, Warrendale, Pennsylvania, 1996.

20. K. H. Leong, et al. "Comparison of YAG and CO2 Laser Welding of Stainless Steels", *Proceedi*
21. K. H. Leong, L. A. Carol and H. N. Bransch. "Welding with High Power CO2 and Nd:YAG Lasers" *Industrial Laser Review*, June 1994.
22. Smithells, C., editor, *Smithells Metals Reference Book*, Butterworths, London, 1983.
23. B. Altshuller, *Personnal Communication*, 1997.
24. The Aluminum Association, *Aluminum Automotive Alloys*, Washington, D.C., 1995.
25. R. P. Martukanitz and B. Altshuller. "Laser beam welding of aluminum alloy 5754-O using a 3 kW Nd:YAG laser and fiber optic beam delivery." *Proceedings of 15th International Congress on Applications of Lasers & Electro-Optics*, Detroit, October 14-17, 1996.

| | | | | | | | |
|-------|-------|-------|------------|----------|-------|-------|-------|
| Si | Fe | Cu | Mn | Mg | Cr | Zn | Ti |
| 0.20% | 0.35% | 0.15% | 0.20-0.50% | 4.0-5.0% | 0.10% | 0.25% | 0.10% |

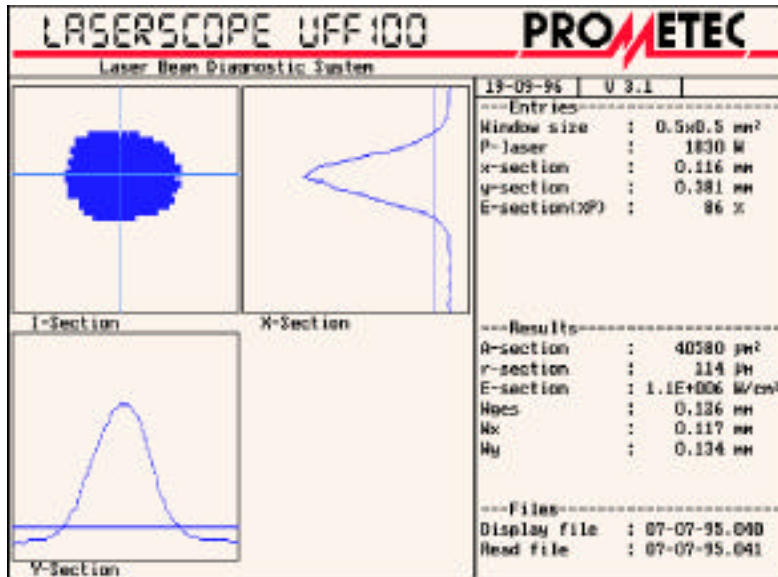
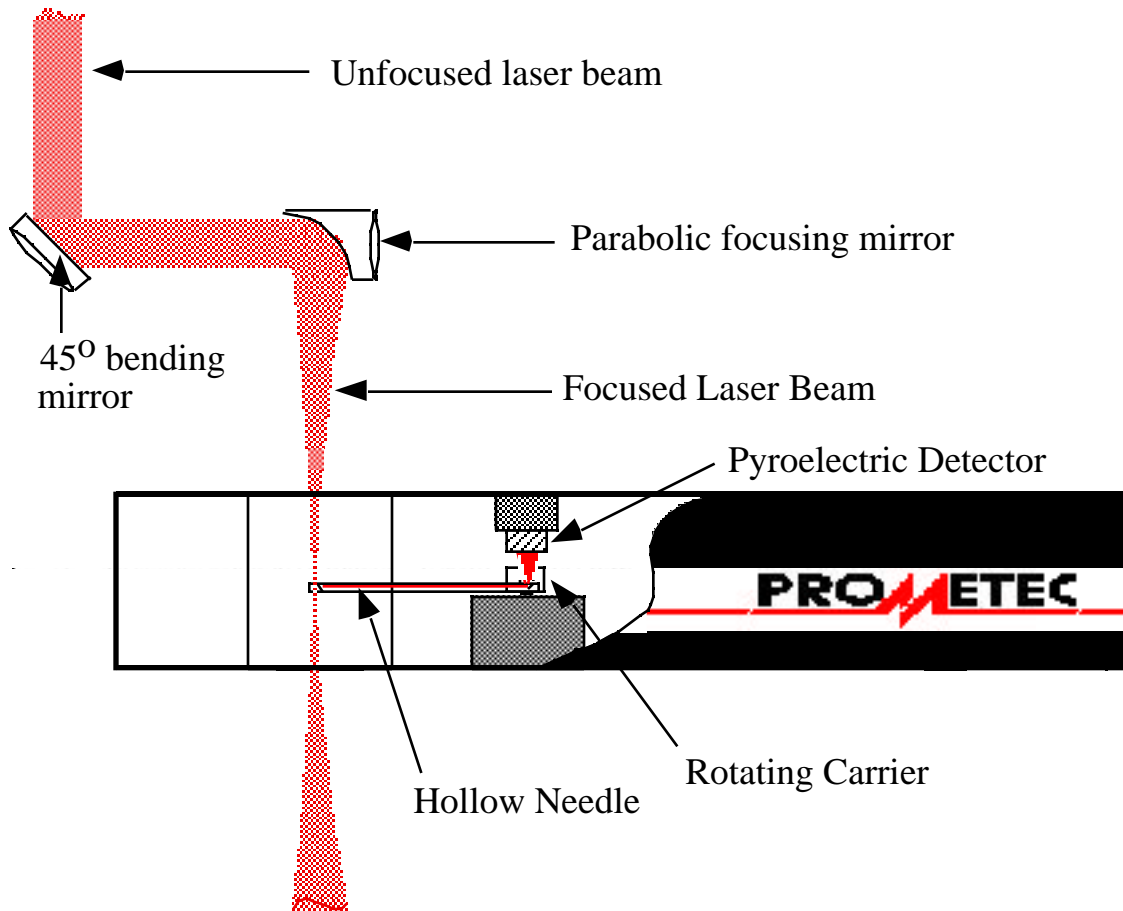
Table 1. Alloying elements in wt. % for the 5182-O aluminum alloy used.

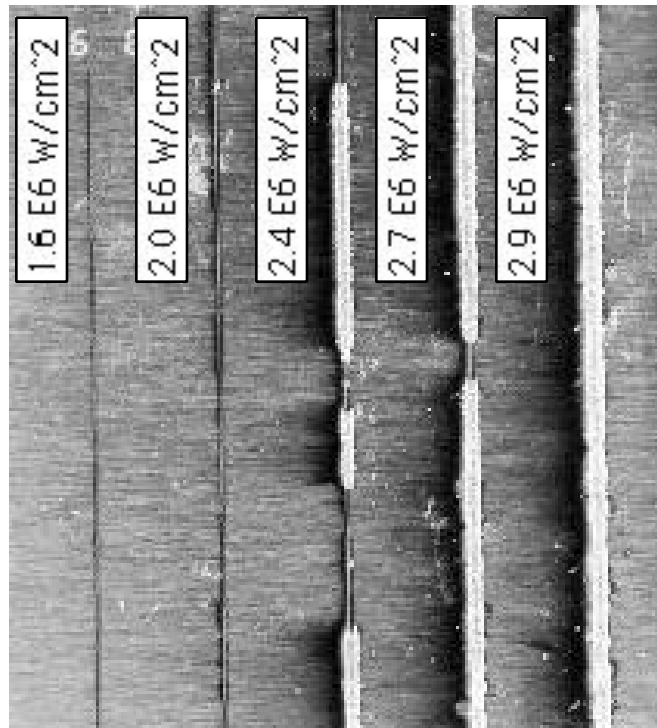
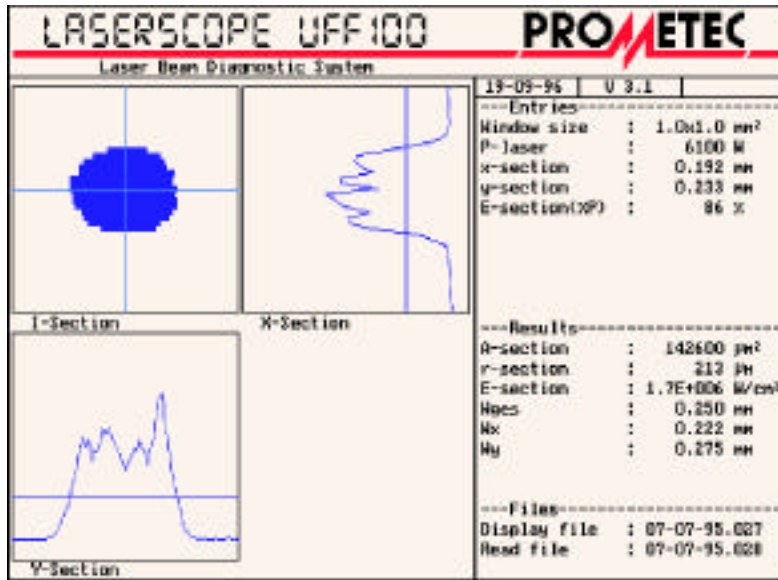
| Weld Type, Region | Wt. % Magnesium | Wt. % Oxygen | Wt. % Aluminum |
|---|-----------------|--------------|----------------|
| 5182 aluminum with cross jet transverse to welding direction. | | | |
| a. Base metal with powder next to weld | 48.3 | 21.5 | 30.2 |
| b. Edge of weld | 14.5 | 8.3 | 77.2 |
| c. Center of weld | 3.0 | 9.8 | 87.1 |
| d. Base metal other side of weld, no powder | 9.7 | 12.4 | 77.9 |
| 5182 aluminum with cross jet pointed at trailing edge of weld pool. | | | |
| a. Base metal with powder next to weld | 3.6 | 26.4 | 43.0 |
| b. Center of weld | 19.1 | 19.0 | 61.9 |
| c. Base metal with powder other side of weld | 14.1 | 18.1 | 67.7 |
| d. Base metal | 9.7 | 11.6 | 78.7 |

Table 2. Energy dispersive x-ray spectroscopy results of weld surfaces.

| Beam Mode | Spot Size (µm) | Sheet Thickness (mm) | No. of Welds | % Welds With Holes |
|-----------|----------------|----------------------|--------------|--------------------|
| 00 | 184-480 | 0.8 | 53 | 40 |
| 20 | 390-520 | 0.8 | 8 | 88 |
| 00 | 184-324 | 1.8 | 24 | 0 |
| 20 | 390-540 | 1.8 | 16 | 0 |

Table 3. Occurrence of cavity defects or holes in welds on 5182 aluminum alloy sheets.





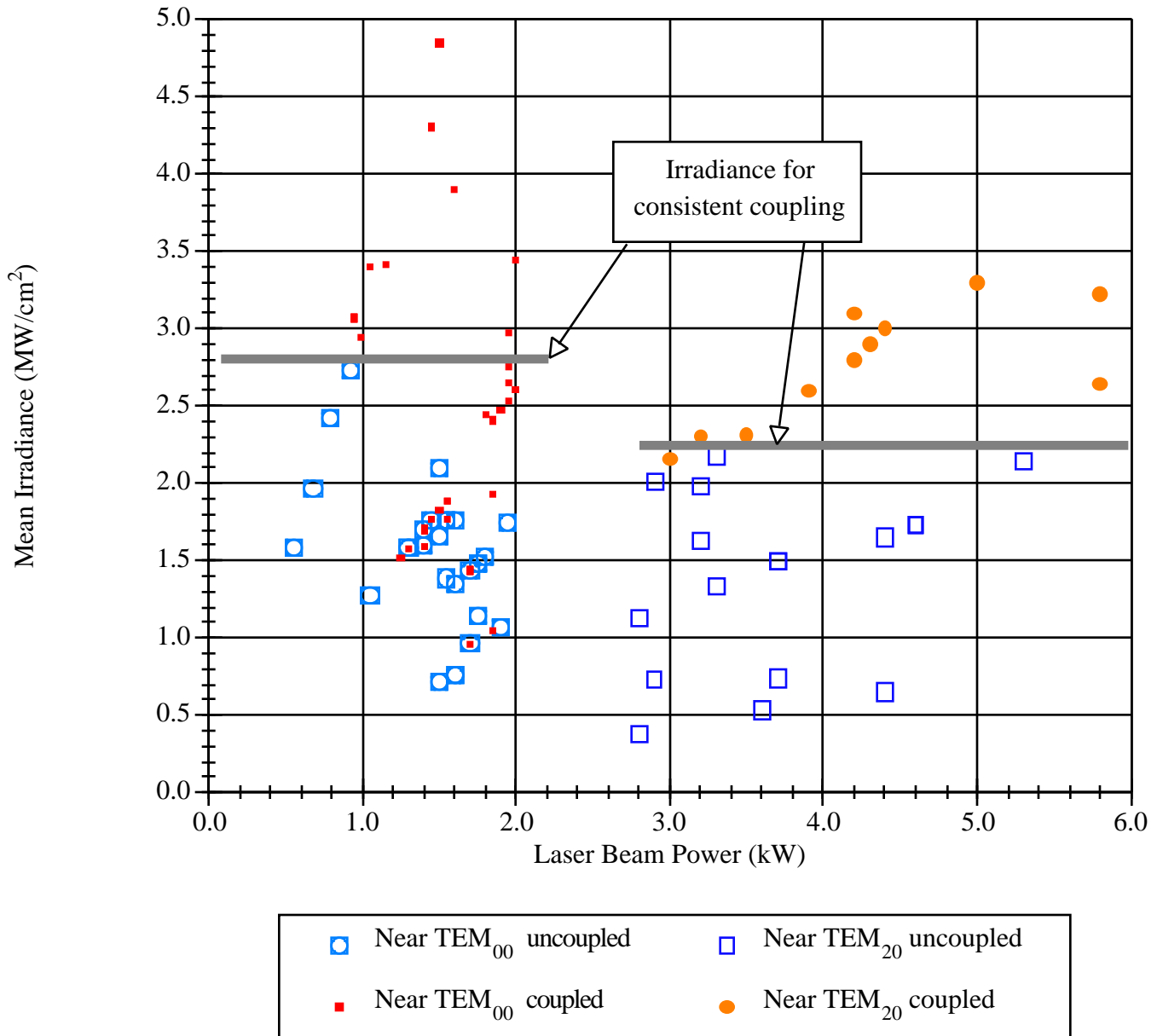
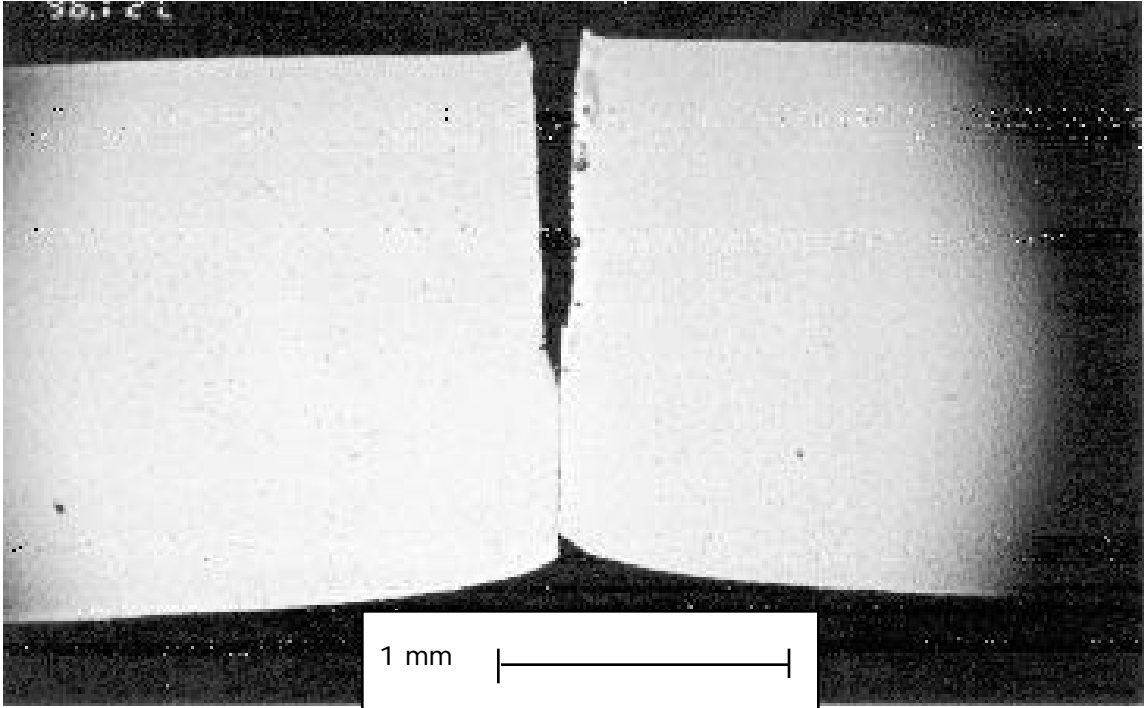
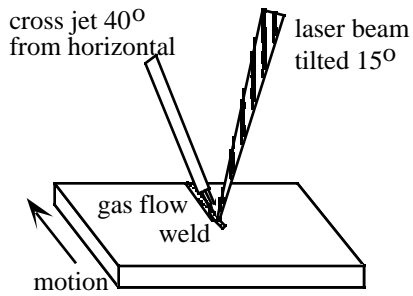
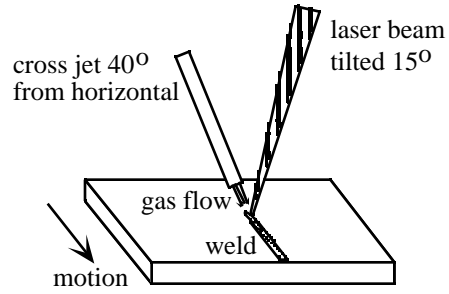


Figure 4. Irradiance data obtained at different beam powers and mode on 5182 aluminum alloy. Consistent welds are indicated by “coupled” and inconsistent and no welds are indicated

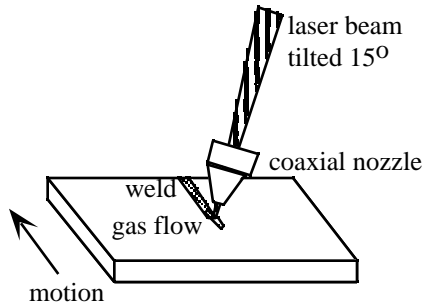




(a) cross jet pointed at leading edge of weld pool



(b) cross jet pointed at trailing edge of weld pool

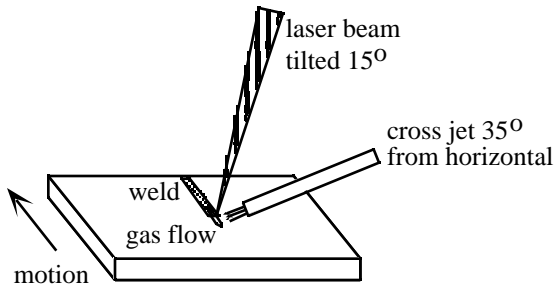


(c) coaxial nozzle

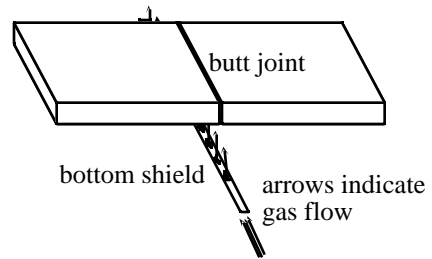


beam exits through 3 mm diameter center hole
gas exits through ring around center hole
and 12 small 1 mm diameter holes surrounding

(d) end view of coaxial nozzle

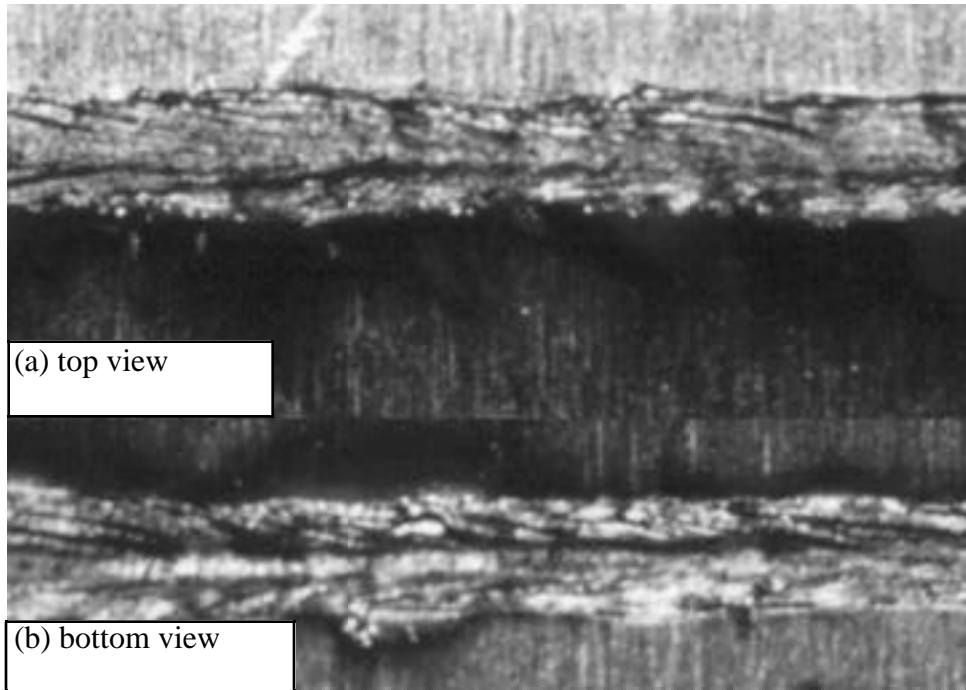
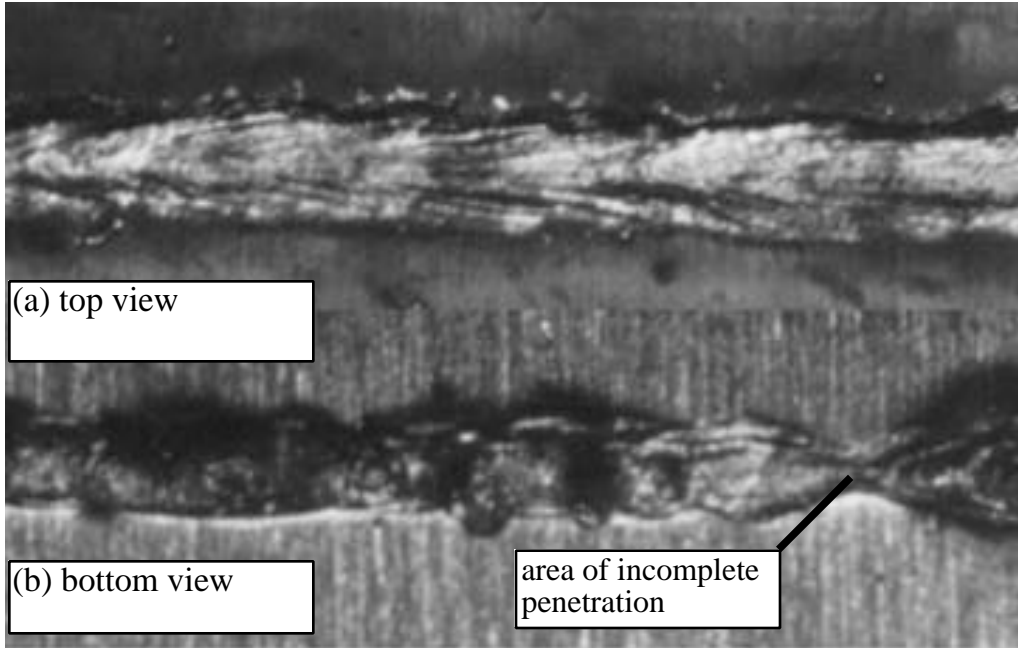


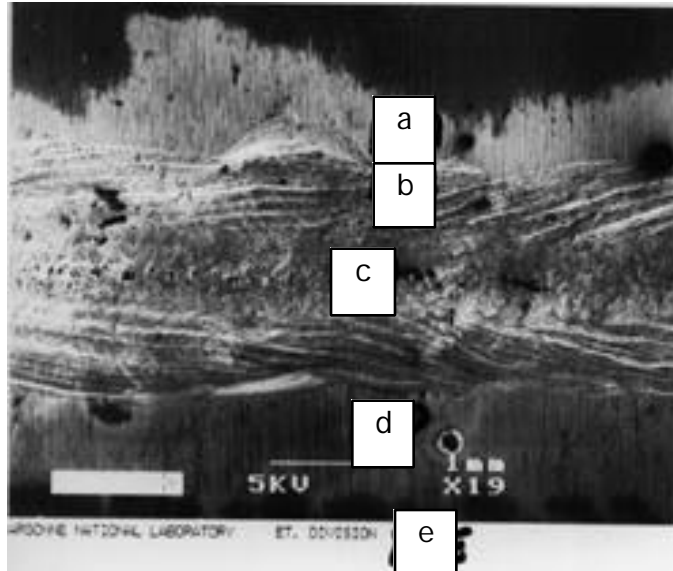
(e) cross jet pointed transverse to welding direction



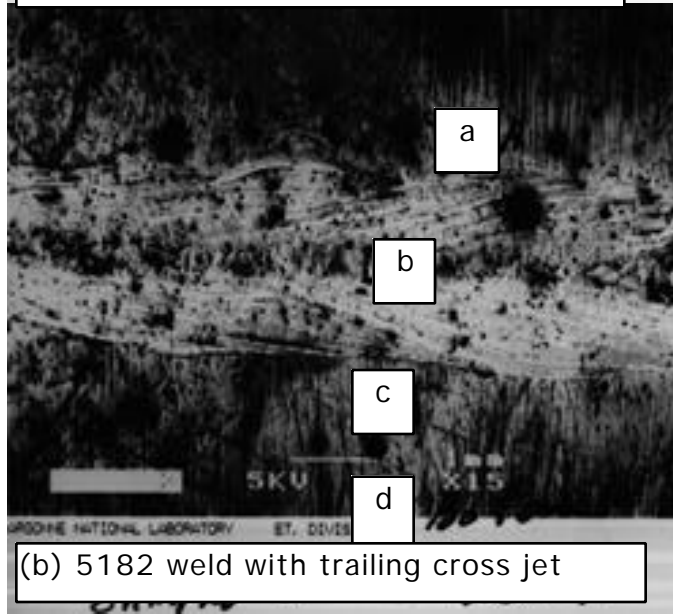
(f) typical bottom shield placement.

Figure 6. Inert gas shielding configurations used for top and bottom of welds.

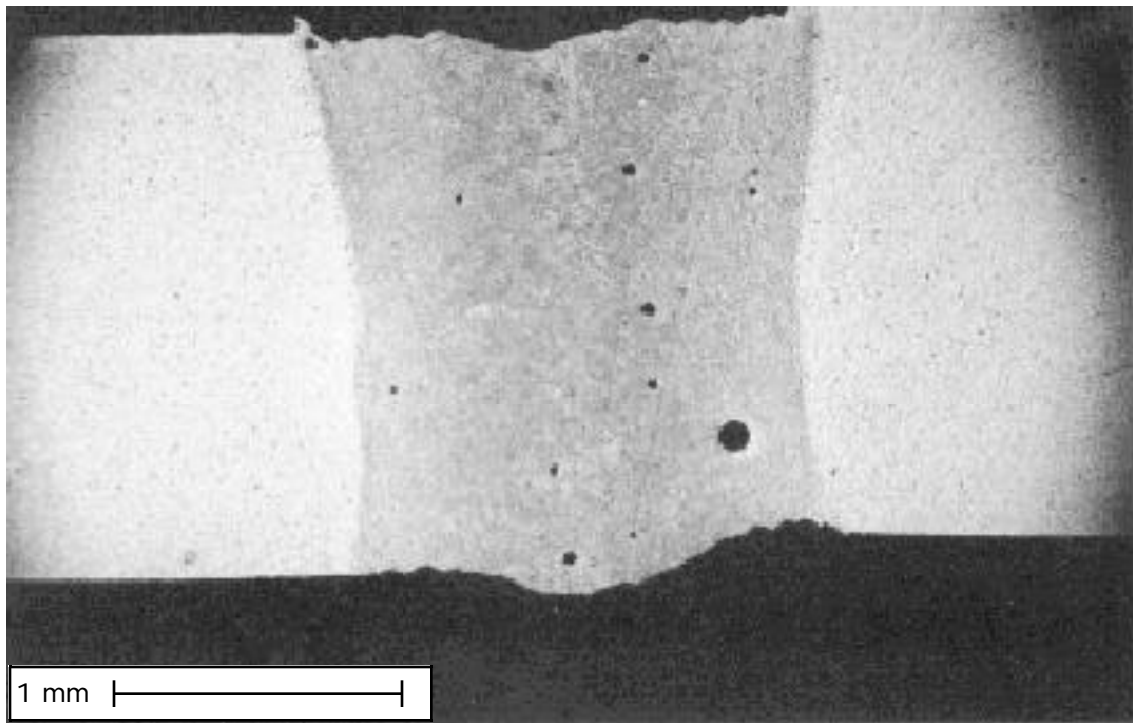
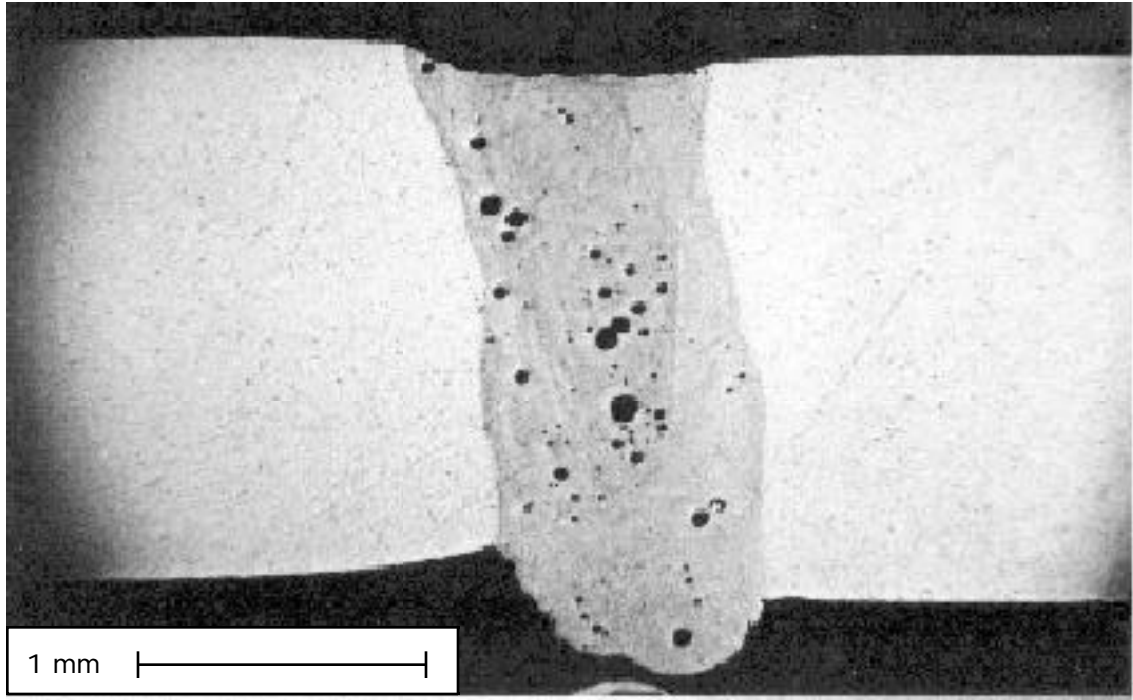




(a) 5182 weld with transverse cross jet



(b) 5182 weld with trailing cross jet



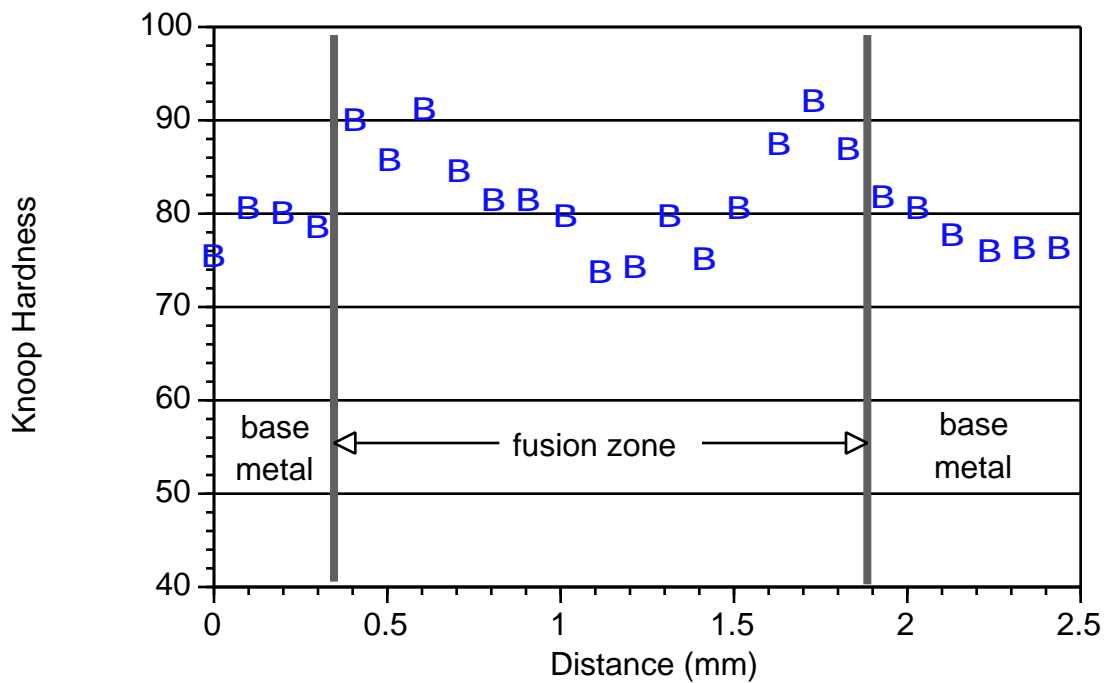


Figure 12. Micro hardness profile of a butt weld made with near TEM₂₀ beam at 4.3 kW, 2.9 MW cm⁻², and 12.7 ms⁻¹.